Diese Arbeit wurde vorgelegt am
Lehr- und Forschungsgebiet Theorie der hybriden Systeme

Optimale Steuerung des Volumenstroms in solarthermischen Parabolrinnenkraftwerken

Optimal Control of Volume Flow in Parabolic Trough Solar Thermal Power Plants

Bachelorarbeit
Informatik

Dezember 2020

Vorgelegt von Presented by	Zeheng Gong Beeckstr. 11 52062 Aachen Matrikelnummer: 378125 zeheng.gong@rwth-aachen.de
Erstprüfer First examiner	Prof. Dr. rer. nat. Erika Ábrahám Lehr- und Forschungsgebiet: Theorie der hybriden Systeme RWTH Aachen University
Zweitprüfer Second examiner	Prof. Dr. rer. nat. Thomas Noll Lehr- und Forschungsgebiet: Software Modellierung und Verifikation RWTH Aachen University
Externer Betreuer External supervisor	Dr. rer. nat. Pascal Richter Steinbuch Centre for Computing Karlsruhe Institute of Technology

Eigenständigkeitserklärung

Hiermit versichere ich, dass ich diese Bachelorarbeit selbständig verfasst und keine anderen als die angegebenen Quellen und Hilfsmittel benutzt habe. Die Stellen meiner Arbeit, die dem Wortlaut oder dem Sinn nach anderen Werken entnommen sind, habe ich in jedem Fall unter Angabe der Quelle als Entlehnung kenntlich gemacht. Dasselbe gilt sinngemäß für Tabellen und Abbildungen. Diese Arbeit hat in dieser oder einer ähnlichen Form noch nicht im Rahmen einer anderen Prüfung vorgelegen.

Aachen, im Dezember 2020

Zeheng Gong

Contents

1 Introduction **1**
- 1.1 State of the art . . . 1
- 1.2 Outline . . . 2

2 Network flow model **3**
- 2.1 Optical model . . . 3
- 2.2 Thermal model . . . 4
  - 2.2.1 Closure equations . . . 6
- 2.3 Hydraulic model . . . 7
- 2.4 Finite volume solver . . . 8

3 PID control **10**
- 3.1 Network model . . . 10
- 3.2 Mirror control . . . 11
- 3.3 Valve control . . . 13

4 Feasibility study **15**
- 4.1 Test case of a parabolic trough power plant . . . 15
- 4.2 Network with single collector row . . . 15
  - 4.2.1 Design point . . . 15
  - 4.2.2 Mirror control . . . 16
  - 4.2.3 Valve control . . . 17
- 4.3 Network with four collector rows . . . 18
  - 4.3.1 Design point . . . 18
  - 4.3.2 Mirror control . . . 19
  - 4.3.3 Valve control . . . 20

5 Conclusion **22**

References **23**

1 Introduction

Electricity generation from conventional fossil fuels like coal and gas causes pollution of air, water and land. Compared with conventional energy sources, solar energy is safe and clean, as it produces no carbon emissions. Thus, it is beneficial to use solar power to generate electricity to restrict climate change. Besides that, solar power has many benefits, as solar thermal energy can be stored quite inexpensively. To meet the future goal that solar power can replace conventional fossil fuels, solar thermal power plants have to generate enough electricity as least as beneficial as fossil-fired plants. Based on different ways of concentrating solar energy, there are solar thermal technologies like solar parabolic trough plants, solar tower power plants, and solar dish power plants. This thesis will focus on parabolic trough plants, which consist of a network of absorber tubes. The tubes heat the contained heat transfer fluid by direct solar irradiation, concentrated via parabolic mirrors. A heat exchanger generates steam with the fluid, and electricity is being generated through a turbine, which is similar to conventional power plants.
The temperature of fluid depends on two factors: direct solar irradiation and mass flow. The more slowly the mass flow passes through the tube, the longer time it is heated up by sunbeams, and therefore it reaches a higher temperature. It is crucial to control the fluid in a specific temperature interval, especially never exceed a specifically defined desired temperature. Otherwise, the fluid will be lead to an irreversible decomposition.

1.1 State of the art

With the increasing popularity of solar energy, there has already been much research on the topic of solar thermal power plants. Researches concerning used materials in power plants, such as mirrors and tubes, has been done [9]. The used materials have been analyzed and evaluated by observation on heat loss [20] and the heat transfer fluid [15, 16]. Design criteria to decrease the construction costs, as well as the best location to construct a solar thermal power plant, have been analyzed [18, 2]. Several kinds of research of controlling the temperature in solar thermal power plants have been made [3]. Approaches as Lyapunov estimator [14, 21], instantaneous control [6, 11] or model predictive control [8, 22] are applied to solar thermal power plants. Most of these control strategies focus on control the temperature of the fluid in a single tube by changing the volume flow of the pump. Hence, the current technology used in controlling parabolic trough solar thermal power plants is mainly used to avoid variations in the temperature. The desired outlet temperature is reached more reliably, and therefore the efficiency of the power plant system is increased. Additionally, to minimize the time and number of defocused mirrors by controlling the valves at each inlet of an absorber tube [5, 23] can maximize the plants' efficiency as well.

This thesis follows the approach by modelling the flow of the fluid through the tubes, considering the pressures in the tubes. The temperature of the fluid will be simulated as a partial differential equation (short: PDE), thereby its value to be regulated at the

end of absorber tubes using valves. With regard to this model, the film temperatures [19], featuring the boundary layer between the fluid and pipe, is also considered. After the description of the flow through the network of tubes, the system will be decoupled such that each tube can be controlled independently.

1.2 Outline

This thesis is structured as follows: Section 2 deals with the modelling of a solar power plant, considering the optics of the solar field, the thermodynamics in the tubes, and the flow in a network of tubes. Section 3 reviews mirror control and valve control, which control the temperature in a network of tubes using proportional-integral-differential (short: PID) controller. The mathematical modelling and optimal control are set up as a Matlab code. At the end of the thesis, the optimal model is tested. The results and evaluation of this feasibility study are presented in Section 4 before the conclusion and outlook are given in Section 5.

2 Network flow model

A parabolic trough solar thermal power plant works as follows: The parabolic mirrors concentrate sun beams onto an absorber tube so that the fluid in the tube is heated up and transports the heat to a heat exchanger. The heat exchanger heated a massive basin of water, the resulting steam powers the turbine, and the generator generates electricity.
The solar thermal power plant consists of two parts, the solar collector field, and the power block, see Figure 1. The solar collector field consists of a network of tubes. The absorber tubes are surrounded by large parabolic mirrors that track the sun and thereby heat the fluid inside them. The well-insulated tubes leading to and from the network are called the inflow and outflow header tubes. They can maintain the temperature of the fluid inside the tube. A pump at the entry of the inflow header tube regulates the volume of the fluid and distributes the heat transfer fluid into the absorber tubes. A fixed valve aperture at the entry of each absorber tube distributes the mass flow uniformly.
This thesis is based on a model by Cherek, that described in this section. An optical model is derived, which represents the energy input from the sun. This model is then used to describe the thermodynamic flow through the network of tubes mathematically.

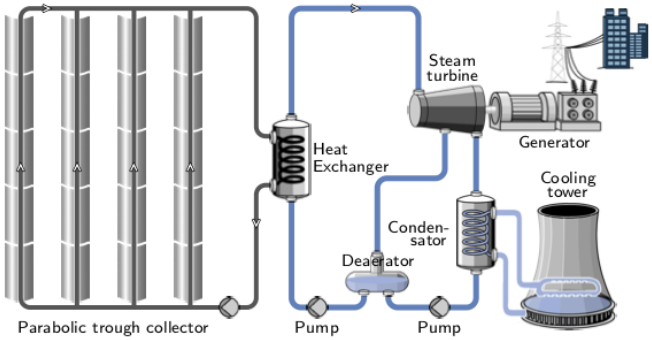

Figure 1: Conceptual drawing of a parabolic trough solar thermal power plant.

2.1 Optical model

The optical model represents the energy input from solar irradiation, which is simulated by a function $I_{\mathrm{DNI}}(x,t)$, dependent on space and time. The environmental characteristics, the geometrical parameters of the collector field, and the parameters describing the parabolic mirrors are considered in the optical model. The incidence angle θ represents the angle between the solar beam and the normal on the surface of the parabolic mirrors. The zenith angle ω represents the angle between the solar beam and the normal on the horizontal surface.The parabolic mirrors with an aperture

width of G reflect the direct solar irradiation $I_{\text{DNI}}(x,t)$. The defocus boolean factor $\phi(x,t) \in \{0,1\}$ states whether the mirror at position x is defocused or broken in time step t. The optical power is concentrated on a cross-sectional area of the absorber tubes, denoted as A_{absorber}. Thus, the volumetric power density into the absorber tube is given by [4],

$$\varphi_{\text{absorber}}(x,t) = \frac{1}{A_{\text{absorber}}} \cdot I_{\text{DNI}}(x,t) \cdot G \cdot \underbrace{\phi(x,t) \cdot \eta_{\text{reflectivity}} \cdot \tau \cdot \alpha \cdot \gamma}_{:=\eta_{\text{opt}}} \cdot \kappa(\theta) \cdot f_{\text{shd}}(x) \cdot f_{\text{end}}(x). \tag{1}$$

where κ is the incidence angle θ modifier, which is used to account for all geometric and optical losses because of an incident angle $\theta > 0°$. Formulas of the incidence angle modifer is given by [17],

$$\kappa(\theta) = \cos(\theta) - 5.25027 \cdot 10^{-4}\theta - 2.859621 \cdot 10^{-5}\theta^2, \tag{2}$$

η_{opt} is the optical efficiency of the collector, which is the product of the optical efficiency of the collector reflectivity $\eta_{\text{reflectivity}}$, the transmittance of the tube metal τ, the absorbance of the absorber tube α, and the intercept factor γ. f_{end} and f_{shd} are two factors due to end loss and row shadowing and can be calculated by [10],

$$f_{\text{end}}(x) = \begin{cases} 0 & \text{if } x \leq d_{\text{focal}} \cdot \tan(\theta) \\ 1 & \text{else,} \end{cases} \tag{3}$$

$$f_{\text{shd}}(x) = \min\left(\max\left(0; \tfrac{\ell_{\text{row}} \cdot \cos(\omega)}{G \cdot \cos(\theta)}\right); 1\right) \tag{4}$$

where ω represents the zenith angle, which is the angle between the solar beam and the normal on the horizontal surface, and θ represents the incidence angle, which is the angle between the solar beam and the normal on the surface of the parabolic mirrors. d_{focal}, ℓ_{row} are the focal distance and row spacing, see Figure 2.

2.2 Thermal model

A model that describes the thermal phenomena of the flow can be constructed based on the conservation law. The energy equation of the absorber tube can be given by [4],

$$\begin{aligned} \frac{\partial}{\partial t} T_{\text{absorber}}(x,t) = & \frac{\varphi_{\text{absorber}}(x,t)}{\rho_{\text{absorber}} \cdot c_{\text{absorber}}} - \frac{\xi^{\text{loss}}_{\text{absorber}} \cdot T_{\text{absorber}}(x,t)}{\rho_{\text{absorber}} \cdot A_{\text{absorber}} \cdot c_{\text{absorber}}} \\ & - \frac{2 \cdot h_{\text{fluid}} \cdot \left(T_{\text{absorber}}(x,t) - T_{\text{fluid}}(x,t)\right)}{\rho_{\text{absorber}} \cdot r_{\text{absorber}} \cdot c_{\text{absorber}}} \end{aligned} \tag{5}$$

where ρ_{absorber}, c_{absorber}, r_{absorber} and A_{absorber} represent the temperature, density, specific heat capacity, radius, and cross-sectional area of the absorber tube. $\varphi_{\text{absorber}}$

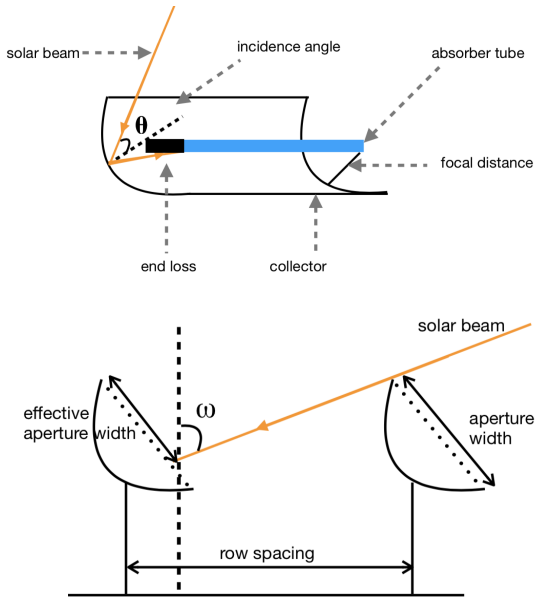

Figure 2: Conceptual drawing of end loss and row shadowing.

represents the volumetric power density into the absorber tube. The heat loss per meter $\xi^{\text{loss}}_{\text{absorber}}$ is the heat loss of the absorber tube per meter, which is caused by the temperature difference between the absorber tube and the exterior glass envelope, and can be simplified as a polynomial in T_{absorber}. h_{fluid} is the convective heat transfer coefficient of the fluid and can be approximated as [7]

$$h_{\text{fluid}} = \frac{\left(\frac{f_{\text{friction}}}{8}\right) \cdot \left(\text{Re}_{\text{absorber}} - 1000\right) \cdot \text{Pr}_{\text{fluid}}}{1 + 12.7 \cdot \left(\frac{f_{\text{friction}}}{8}\right)^{1/2} \cdot \left(\text{Pr}_{\text{fluid}}^{2/3} - 1\right)} \cdot \left(\frac{\text{Pr}_{\text{fluid}}}{\text{Pr}_{\text{absorber}}}\right)^{0.11} \cdot \frac{\lambda_{\text{fluid}}}{2 \cdot r_{\text{absorber}}} \tag{6}$$

with the friction factor for the inner surface of the absorber tube

$$f_{\text{friction}} = \left(1.82 \cdot \log_{10}(\text{Re}_{\text{absorber}}) - 1.64\right)^{-2}$$

where $\text{Re}_{\text{absorber}}$ is the Reynolds number of absorber tube based on its inner surface temperature. Pr_{fluid} and $\text{Pr}_{\text{absorber}}$ are the Prantl number evaluated at the fluid temperature and the absorber inner surface temperature. λ_{fluid} represents the thermal conductivity of the fluid.
The energy equation of the volumetric flow can be given by [4],

$$\frac{\partial}{\partial t} T_{\text{fluid}}(x,t) + \nu_{\text{fluid}} \cdot \frac{\partial}{\partial x} T_{\text{fluid}}(x,t) = \frac{2 \cdot h_{\text{fluid}} \cdot \left(T_{\text{absorber}}(x,t) - T_{\text{fluid}}(x,t)\right)}{\rho_{\text{fluid}} \cdot c_{\text{fluid}} \cdot r_{\text{absorber}}} \tag{7}$$

where r_{absorber} is the radius of the absorber tube. T_{fluid}, ρ_{fluid}, ν_{fluid}, c_{fluid}, h_{fluid} represent the temperature, density, velocity, specific heat capacity and convective heat transfer coefficient of the heat transfer fluid.

Equations (5) - (7) construct the thermal model of the parabolic trough solar thermal power plants. This model is applied to simulate the outlet temperature of the heat transfer fluid.

2.2.1 Closure equations

Therminol VP1 and molten salt are considered as heat transfer fluids for closure equations. Their density, specific heat capacity, thermal conductivity are usually given as polynomials up to degree three, four, two, depending on the temperature T as argument

$$\rho(T) = a_{\rho,0} + a_{\rho,1}T + a_{\rho,2}T^2 + a_{\rho,3}T^3 \tag{8}$$
$$c(T) = a_{c,0} + a_{c,1}T + a_{c,2}T^2 + a_{c,3}T^3 + a_{c,4}T^4 \tag{9}$$
$$\lambda(T) = a_{\lambda,0} + a_{\lambda,1}T + a_{\lambda,2}T^2 \tag{10}$$

see Table 3 for the coefficients of Therminol VP1 [25] and molten salt, and Table 4 for the temperature limits of Therminol VP1 and molten salt [24].

Coefficients for Density $\rho(T)$		
	Therminol VP1	molten salt
$a_{\rho,0}$	1437.78	2293.6
$a_{\rho,1}$	-1.86453	-0.7497
$a_{\rho,2}$	$2.7208 \cdot 10^{-3}$	0
$a_{\rho,3}$	$-2.367 \cdot 10^{-6}$	0

Table 1: The density ρ of Therminol VP1 and molten salt can be expressed as polynomials up to degree three, in dependency of the temperature T as argument.

Coefficients for Specific heat capacity $c(T)$		
	Therminol VP1	molten salt
$a_{c,0}$	2138.06	5806.0
$a_{c,1}$	-11.1303	-10.833
$a_{c,2}$	$5.02177 \cdot 10^{-2}$	$7.2413 \cdot 10^{-3}$
$a_{c,3}$	$-7.81413 \cdot 10^{-5}$	0
$a_{c,4}$	$4.4172 \cdot 10^{-8}$	0

Table 2: The specific heat capacity c of Therminol VP1 and molten salt can be expressed as polynomials up to degree four, in dependency of the temperature T as argument.

The temperature of the fluid has to be maintained in a certain given range $[T_{\text{min}}, T_{\text{crit}}]$. The T_{inlet} and desired temperature T_{desired} are defined for safe operation, as well. Moreover, the performance of the pump is limited to a maximum possible volume flow $q_{\text{pump}}^{\text{max}}$, which usually is chosen such that for high direct solar irradiations of the full mirror focus length can be used.

Coefficients for Thermal Conductivity $\lambda(T)$		
	Therminol VP1	molten salt
$a_{\lambda,0}$	0.1491	0.443
$a_{\lambda,1}$	$7.0218 \cdot 10^{-6}$	$1.9 \cdot 10^{-4}$
$a_{\lambda,2}$	$-1.7246 \cdot 10^{-7}$	0

Table 3: The thermal conductivity λ of Therminol VP1 and molten salt can be expressed as polynomials up to degree two, in dependency of the temperature T as argument.

Temperature limits		
	Therminol VP1	molten salt
T_{min}	285 K	495 K
T_{inlet}	340 K	500 K
T_{desired}	668 K	828 K
T_{crit}	673 K	833 K

Table 4: The minimal, desired and critical temperature of Therminol VP1 and molten salt is given.

2.3 Hydraulic model

The thermal model which is introduced in the last subsection specifies the behavior of the fluid temperature inside the juntions. It has been done by Cherek in his thesis [5]. As an extension of the exsiting model of Cherek, this subsection will present a model that describes the hydraulic phenomena of the flow in the header tubes, which is also constructed based on the conservation law. The momentum equation of the fluid in the tubes can be given by

$$\begin{aligned}&\frac{\partial}{\partial t}\big(\rho_{\text{fluid}}(x,t)\cdot\nu_{\text{fluid}}(x,t)\big)+\frac{\partial}{\partial x}\big(\rho_{\text{fluid}}(x,t)\cdot\nu^2_{\text{fluid}}(x,t)+p_{\text{fluid}}(x,t)\big)\\&=-\frac{\omega_{\text{absorber}}}{D_{\text{absorber}}}\cdot\ell_{\text{absorber}}\cdot\frac{\rho_{\text{fluid}}(x,t)\cdot\nu_{\text{fluid}}(x,t)\cdot|\nu_{\text{fluid}}(x,t)|}{2}+\frac{4}{3}\cdot\frac{\partial}{\partial x}\big(\mu_{\text{fluid}}(x,t)\cdot\frac{\partial}{\partial x}\nu_{\text{fluid}}(x,t)\big)\end{aligned}\tag{11}$$

where $\rho_{\text{fluid}}(x,t)$, $\nu_{\text{fluid}}(x,t)$, $p_{\text{fluid}}(x,t)$, $\mu_{\text{fluid}}(x,t)$ represent the density, velocity, pressure, dynamic viscosity of the fluid at position x in time step t, respectively. ω_{absorber}, D_{absorber} and ℓ_{absorber} are the surface roughness, diameter and length of the absorber tube. The last part of equation (11) has a very small impact on the results and can be neglected [5], which yields

$$\begin{aligned}&\frac{\partial}{\partial t}\big(\rho_{\text{fluid}}(x,t)\cdot\nu_{\text{fluid}}(x,t)\big)+\frac{\partial}{\partial x}\big(\rho_{\text{fluid}}(x,t)\cdot\nu^2_{\text{fluid}}(x,t)+p_{\text{fluid}}(x,t)\big)\\&=-\frac{\omega_{\text{absorber}}}{D_{\text{absorber}}}\cdot\ell_{\text{absorber}}\cdot\frac{\rho_{\text{fluid}}(x,t)\cdot\nu_{\text{fluid}}(x,t)\cdot|\nu_{\text{fluid}}(x,t)|}{2}\end{aligned}\tag{12}$$

2.4 Finite volume solver

The energy equations (5) and (7) can be solved numerically by finite volume method using Godunov splitting. First, the homogenous part of the partial differential equation (7) can be solved by

$$\frac{\partial}{\partial t} T_{\text{fluid}}(x,t) + \nu_{\text{fluid}} \cdot \frac{\partial}{\partial x} T_{\text{fluid}}(x,t) = 0 \tag{13}$$

As the flow velocity ν is always positive, the HTF flows in the positive x-direction. Hence, it is practical to use an upwind scheme with spatial discretization Δx, and temporal discretization Δt to solve the equation,

$$\begin{aligned} &C_i = \left(x_{i-\frac{1}{2}}, x_{i+\frac{1}{2}} \right), \\ &x_i = i \cdot \Delta x, \quad i = 0, \ldots, N_x \in \mathbb{N}, \quad \text{and} \quad t_n = n \cdot \Delta t, \quad n = 0, \ldots, N_t \in \mathbb{N}. \end{aligned} \tag{14}$$

The update step of cell C_i for the time step from $t_n \to t_{n+1}$ is given by

$$T_{\text{fluid}}(i, t_{n+1}^{-}) = T_{\text{fluid}}(i, t_n) - \Delta t \cdot \left(\nu_{\text{fluid}} \cdot \frac{T_{\text{fluid}}(i, t_n) - T_{\text{fluid}}(i-1, t_n)}{\Delta x} \right) \tag{15}$$

where the indices i represents the cell index and n represents the current time step. In the same way as above, the energy equation of absorber tube (5) can be solved by

$$\begin{aligned} T_{\text{absorber}}(i, t_{n+1}^{=}) = &T_{\text{absorber}}(i, t_n) - \Delta t \cdot \left(\frac{\varphi_{\text{absorber}}(i, t_n)}{\rho_{\text{absorber}} \cdot c_{\text{absorber}}} - \frac{\xi_{\text{absorber}}^{\text{loss}} \cdot T_{\text{absorber}}(i, t_n)}{\rho_{\text{absorber}} \cdot A_{\text{absorber}} \cdot c_{\text{absorber}}} \right. \\ &\left. - \frac{2 \cdot h_{\text{fluid}} \cdot \left(T_{\text{absorber}}(i, t_n) - T_{\text{fluid}}(i, t_n) \right)}{\rho_{\text{absorber}} \cdot r_{\text{absorber}} \cdot c_{\text{absorber}}} \right) \end{aligned} \tag{16}$$

Then the source terms can be taken into account by solving the ordinary differential equation

$$\frac{\partial}{\partial t} T_{\text{fluid}}(x,t) = \frac{2 \cdot h_{\text{fluid}} \cdot \left(T_{\text{absorber}}(x,t) - T_{\text{fluid}}(x,t) \right)}{\rho_{\text{fluid}} \cdot c_{\text{fluid}} \cdot r_{\text{absorber}}} \tag{17}$$

which yields

$$T_{\text{fluid}}(i, t_{n+1}) = T_{\text{fluid}}(i, t_{n+1}^{-}) + \Delta t \cdot \left(\frac{2 \cdot h_{\text{fluid}} \cdot \left(T_{\text{absorber}}(i, t_{n+1}^{=}) - T_{\text{fluid}}(i, t_{n+1}^{-}) \right)}{\rho_{\text{fluid}} \cdot c_{\text{fluid}} \cdot r_{\text{absorber}}} \right) \tag{18}$$

Analogously as in the thermal model, the momentum equation (12) can be solved numerically using Godunov splitting. The update step of cell C_i for the time step from

$t_n \to t_{n+1}$ is given by

$$\rho_{\text{fluid}}(i, t_{n+1}^-) \cdot \nu_{\text{fluid}}(i, t_{n+1}^-) = \rho_{\text{fluid}}(i, t_n) \cdot \nu_{\text{fluid}}(i, t_n) - \frac{\Delta t}{\Delta x} \cdot \left(\rho_{\text{fluid}}(i, t_n) \cdot \nu_{\text{fluid}}^2(i, t_n) - (\rho_{\text{fluid}}(i-1, t_n) \cdot \nu_{\text{fluid}}^2(i-1, t_n) + p_{\text{fluid}}(i, t_n) - p_{\text{fluid}}(i-1, t_n) \right) \tag{19}$$

where the indices i represents the cell index and n represents the current time step. Then the loss terms can be taken into account by solving the ordinary differential equation

$$\frac{\partial}{\partial t}(\rho_{\text{fluid}} \cdot \nu_{\text{fluid}})(x, t) = -\frac{\omega_{\text{absorber}}}{D_{\text{absorber}}} \cdot \ell_{\text{absorber}} \cdot \frac{\rho_{\text{fluid}}(x, t) \cdot \nu_{\text{fluid}}(x, t) \cdot |\nu_{\text{fluid}}(x, t)|}{2} \tag{20}$$

which can be given by

$$\begin{aligned} &\rho_{\text{fluid}}(i, t_{n+1}) \cdot \nu_{\text{fluid}}(i, t_{n+1}) \\ &= \rho_{\text{fluid}}(i, t_{n+1}^-) \cdot \nu_{\text{fluid}}(i, t_{n+1}^-) \\ &+ \Delta t \cdot \left(- \frac{\omega_{\text{absorber}}}{D_{\text{absorber}}} \cdot \ell_{\text{absorber}} \cdot \frac{\rho_{\text{fluid}}(i, t_{n+1}^-) \cdot \nu_{\text{fluid}}(i, t_{n+1}^-) \cdot |\nu_{\text{fluid}}(i, t_{n+1}^-)|}{2} \right) \end{aligned} \tag{21}$$

Since $\rho_{\text{fluid}}(i, t_n) = \rho(T_{\text{fluid}}(i, t_n))$, the velocity of the fluid $\nu_{\text{fluid}}(i, t_n)$ in the cell C_i at time step t_n can be simply computed by

$$\nu_{\text{fluid}}(i, t_n) = \frac{\rho_{\text{fluid}}(i, t_n) \cdot \nu_{\text{fluid}}(i, t_n)}{\rho_{\text{fluid}}(T_{\text{fluid}}(i, t_n))}. \tag{22}$$

3 PID control

In this section, the current state of the art control with a proportional–integral–derivative (PID) controller, which changes the pump's volume flow, will be presented. The standard PID controller changes the pump's volume flow and defocuses mirrors from the collector field, so that the outflow temperature of each absorber tube is as close as possible to the desired temperature. The desired temperature T_{desired} and a threshold around it have to be defined for each specific HTF. Moreover, the temperature in the absorber tubes has to be prevented decrease too much. The defocussing of mirrors causes loss of energy input, which means lower efficiency. Hence, an advanced PID controller, which additionally controls the flow in each tube will be introduced. The system of tubes is decoupled, to control each absorber tube independently. By setting the aperture of the valves, the volumetric flow in a single absorber tube can be controlled without influencing the volumetric flow of the other tubes. The valve control allows us to decrease the defocus time of the mirrors to zero when the outflow temperature is controlled in the interval of the threshold around the desired temperature. The efficiency of the solar thermal power plant is increased because of the minimization of the defocus time of mirrors in the collector field. The PID control, which is described in this section, is fundamentally based on Cherek's Thesis [5].

3.1 Network model

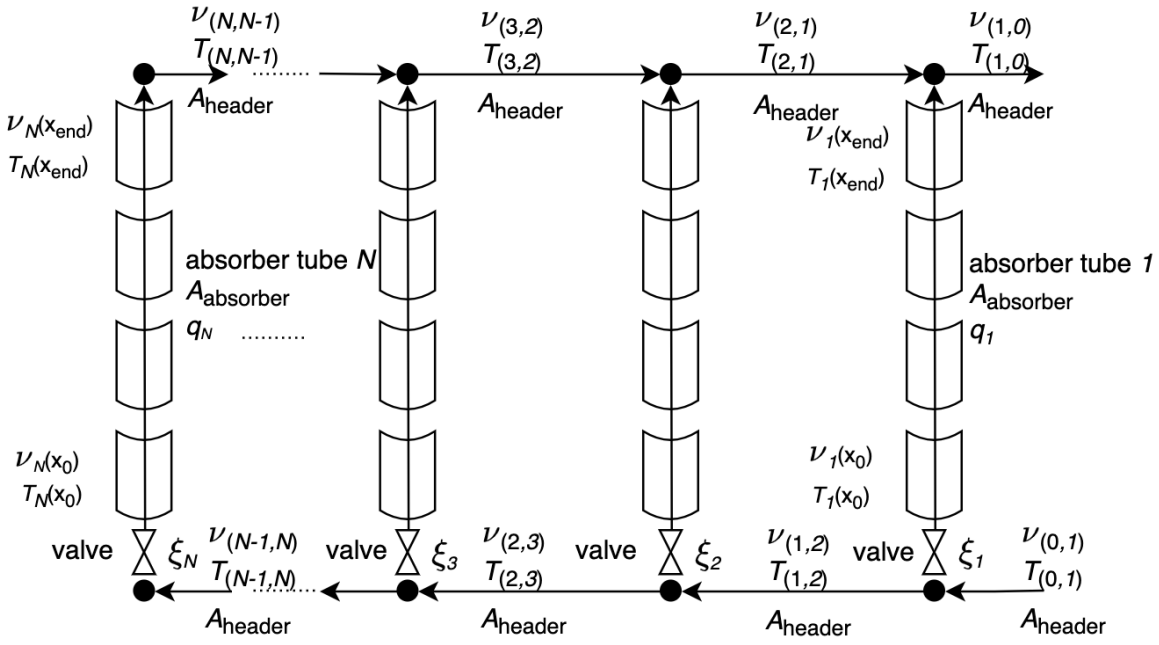

Figure 3: Conceptual drawing of a network of tubes.

The overall fluid distributes into the parallel absorber tubes. An absorber tube with numbering $k = 1, ...N$ has valve's aperture ξ_k. The fluid in the absorber k has velocity ν_k, volume flow q_k, temperature T_k. All absorber tubes have cross sectional area A_{absorber} and they are connected with the header tubes with cross sectional area A_{header}. The edge of the inflow header tube between the two junctions of absorber tube k and $k+1$ is denoted by $(k, k+1)$, with flow velocity $\nu_{(k,k+1)}$, volume flow $q_{(k,k+1)}$, and temperature $T_{(k,k+1)}$. The edge of the outflow header tube is denoted by $(k+1, k)$, see Figure 3.
The junctions that connect the inflow header tube and the absorber tubes are denoted as inlet junctions, whereas the junctions that connect the outflow header tube and the absorber tubes are denoted as outlet junctions.
At each inlet junction, a valve with aperture $\xi_k \in [0, 1]$ controls the absorber tube's volume flow, where 0 means fully closed and 1 means fully opened. The temperature changes along the inflow header tube are neglected, thus

$$T_k(x_0) := T_{(k-1,k)} \quad \text{and} \quad T_{(k,k+1)} := T_{(k-1,k)} \tag{23}$$

At each outlet juntion, the outflow temperature of the fluid can be computed by using Richmann's calorimetric mixing formula [1],

$$T_{(k,k-1)} = \frac{\rho_{(k+1,k)} \cdot \nu_{(k+1,k)} \cdot c_{\nu,(k+1,k)} \cdot T_{(k+1,k)} + \rho_k \cdot \nu_k \cdot A_{\text{absorber}} \cdot c_{\nu,k} \cdot T_k(x_{end})}{\rho_{(k+1,k)} \cdot \nu_{(k+1,k)} \cdot c_{\nu,(k+1,k)} + \rho_k \cdot \nu_k \cdot A_{\text{absorber}} \cdot c_{\nu,k}} \tag{24}$$

3.2 Mirror control

The standard PID control, which only changes the pump's volume flow and defocuses mirrors, is called mirror control. The network in a solar thermal power plant is set to a design point yearly. The idea behind the design point is to calibrate the valves to an ideal point so that as many as possible mirrors are being used. The valves' apertures are kept constant until the next calibration. The design point is calculated on the condition that the solar irradiation is constant in all absorber tubes. Therefore, the volumetric flow of the design point q_{DP} in each tube has to be equal. It depends on the length of the absorber tube ℓ_{absorber}, the solar irradiation at the design point $I_{\text{DNI,DP}}$, the inflow temperature T_{in}, and the desired temperature T_{desired}. The design point is considered as a steady state, which means $\frac{\partial T}{\partial t} = 0$. From the equation (7) we have

$$\nu_{\text{fluid}} \cdot \frac{\partial}{\partial x} T_{\text{fluid}}(x,t) = \frac{2 \cdot h_{\text{fluid}} \cdot \big(T_{\text{absorber}}(x,t) - T_{\text{fluid}}(x,t)\big)}{\rho_{\text{fluid}} \cdot c_{\text{fluid}} \cdot r_{\text{absorber}}} \tag{25}$$

Since $\nu_{\text{fluid}} \cdot A_{\text{absorber}} = q_{\text{DP}}$,

$$q_{\text{DP}} \cdot \frac{\partial}{\partial x} T_{\text{fluid}}(x,t) = \frac{2 \cdot h_{\text{fluid}} \cdot A_{\text{absorber}} \cdot \big(T_{\text{absorber}}(x,t) - T_{\text{fluid}}(x,t)\big)}{\rho_{\text{fluid}} \cdot c_{\text{fluid}} \cdot r_{\text{absorber}}} \tag{26}$$

The temperature derivative can be approximated as the simple central difference between the temperature at the inflow T_{in} and the desired temperature at the outflow T_{desired} of each absorber tube,

$$\frac{\partial}{\partial x} T_{\text{fluid}}(x,t) = \frac{T_{\text{desired}} - T_{\text{in}}}{\ell_{\text{absorber}}}. \tag{27}$$

The solar irradiation $I_{\text{DNI}}(x,t)$ is set to

$$I_{\text{DNI}}(x,t) = I_{\text{DNI,DP}}. \tag{28}$$

The density ρ_{fluid} and specific heat capacity c_{fluid} are assumed as

$$\begin{aligned} \rho_{\text{fluid}} &= \rho_{\text{DP}}, \\ c_{\text{fluid}} &= c_{\text{DP}} \end{aligned} \tag{29}$$

and can be computed iteratively.
Combining equations (26) and (27) we get

$$q_{\text{DP}} = \frac{2 \cdot \ell_{\text{absorber}} \cdot h_{\text{fluid}} \cdot A_{\text{absorber}} \cdot \left(T_{\text{absorber}}(x,t) - T_{\text{fluid}}(x,t)\right)}{\rho_{\text{fluid}} \cdot c_{\text{fluid}} \cdot r_{\text{absorber}} \cdot (T_{\text{desired}} - T_{\text{in}})} \tag{30}$$

The volumetric flow for the pump at the design point $q_{\text{pump,DP}}$ can be represented as the multiplication of the volumetric flow in a single absorber tube q_{DP} with the total number of absorber tubes N,

$$q_{\text{pump,DP}} = N \cdot q_{\text{DP}} \tag{31}$$

The valves are set to distribute the volumetric flow of the pump $q_{\text{pump,DP}}$ evenly through all absorber tubes so that q_{DP} can be reached in every single absorber tube.

Mirror control is the control of the pump and the defocussing of mirrors. By decreasing the pump volumetric flow q_{pump}, the HTF has a longer time to heat up so that its temperature increases. A PID-controller designed with the Ziegler-Nichols tuning method [13] is used to control the pump volumetric flow q_{pump} with the temperature derivation ΔT_{fluid} at the end of the absorber tube. the differential equation for the controller is

$$q_{\text{pump}}(t_{n+1}) = K_p \cdot \left(\Delta T_{\text{fluid}} + \frac{1}{T_i} \int \Delta T_{\text{fluid}} dt + T_d \cdot \frac{\partial(\Delta T_{\text{fluid}})}{\partial t} \right). \tag{32}$$

The parameters K_p, T_i and T_d are chosen by Table 5. The integral and derivative gains have to be set to zero at first. Then, the proportional gain K_p is set to zero and slowly increased until the output and of the control loop shows stable and consistent oscillations. K_u is set to the obtained proportional gain and T_u to the oscillation period of the output.

K_p	T_i	T_d
$0.6K_u$	$T_u/2$	$T_u/8$

Table 5: Chosen parameters for the Ziegler-Nichols method [5]

The volumetric flow of the pump q_{pump} is distributed evenly into each single absorber tube. Hence, in order to achieve the needed volumetric flow in the i-th absorber tube, the difference between the old and new volumetric flow in the i-tube is added to the pump volumetric flow multiplied by the total number of absorber tubes in the solar thermal power plant N,

$$q_{\text{pump}}(t_{n+1}) = q_{\text{pump}} + (q_i(t_{n+1}) - q_i(t_n)) \cdot N. \tag{33}$$

In order to ensure that the desired temperature T_{desired} will not be exceeded, mirrors are being defocused. The number of mirrors that have to be defocused N_{defocus} is computed by

$$N_{\text{defocus}} = \left\lceil \frac{\Delta T_{\text{desired}}}{\Delta T_{\text{mirror}}} \right\rceil \tag{34}$$

where ΔT_{mirror} is the increase in temperature over the length of one mirror in an absorber tube and $\Delta T_{\text{desired}}$ is the difference between the current temperature and the desired temperature. The algorithm for defocusing mirrors is shown in Algorithm 1.

Algorithm 1 Mirror Control

```
for tube i = 1; i ≤ N; i++ do
    if T_i < T_desired then
        decrease overall volumetric flow q_P;
    end if
end for
for tube i = 1; i ≤ N; i++ do
    if T_i > T_desired then
        calculate N_defocus;
        defocus mirrors;
    end if
end for
```

3.3 Valve control

Since every defocused mirror causes a loss of input energy, the defocus time of mirrors in the collector field must be minimized. The valve control, which uses the valves dynamically in the control process, is introduced in this subsection. It is designed to decrease the defocus time of mirrors to zero while keeping the HTF's temperature in the threshold's interval around the desired temperature. The tubes' system is decoupled

so that the volumetric flow of each single absorber tube of the network can be changed independently by setting the aperture of the valves.

The decoupling of the volume flows in the individual pipes is derived by the following formula

$$q_k = q_{\text{pump}} \cdot \left(1 - \frac{A_{\text{absorber}} \cdot \sum_{i=1, i\neq k}^{N} \xi_i}{A_{\text{absorber}} \cdot \sum_{i=1}^{N} \xi_i}\right) \quad \forall \quad n \in \{1, ..., N\} \tag{35}$$

where q_k is the volume flow in absorber tube k, and ξ_k is the aperture of the valve k.

In every iterative process, the interdependence between the valves can be constructed as a matrix equation of Q, Xi, A_{absorber}, and q_{pump}, where Q is a 1-by-N matrix with elements q_i, $i \in \{1, ..., N\}$:

$$\mathrm{Q} = \begin{pmatrix} q_1 & q_2 & \dots & q_N \end{pmatrix}, \tag{36}$$

Xi is a 1-by-N matrix with elements ξ_i, $i \in \{1, ..., N\}$:

$$\mathrm{Xi} = \begin{pmatrix} \xi_1 & \xi_2 & \dots & \xi_N \end{pmatrix} \tag{37}$$

such that

$$q_{\text{pump}} \cdot \left(1 - \frac{A_{\text{absorber}} \cdot \mathrm{Xi} \cdot (\mathrm{I} - e_i)}{A_{\text{absorber}} \cdot \mathrm{Xi} \cdot \mathrm{I}}\right) - \mathrm{Q} \cdot e_i = 0 \tag{38}$$

where e_i are the standard unit vectors of dimension $\mathbb{R}^N$ with one as the i-th element , I is a N-by-1 matrix of ones. As the other parameters are given, the matrix equation (38) can be solved for Xi. Thus, each valve's aperture can be obtained. According to the equation (7), the velocity ν has to be positive. Hence, a minimum aperture of the valves has to be defined,

$$\xi_i > \xi_{\text{min}} \quad \forall \quad n \in \{1, ..., N\} \tag{39}$$

Algorithm 2 below computes the valves' opening state so that the added volumetric flow only affects the particular absorber tube.

Algorithm 2 Valves Aperture

1: $q_{diff} = q_k - q_{old,k}$;
2: $q_{\text{pump}} = q_{\text{pump}} + q_{diff}$;
3: **for** i=1; i<N; i++ **do**
4: update ξ_i by equation (38);
5: **end for**

4 Feasibility study

In this section, the introduced controlling method are examined in a test case with several EuroTrough 150 tubes in a row [12]. The test case consists of a network of four absorber tube and will involve shadowing of the collectors, see Table 6.

4.1 Test case of a parabolic trough power plant

The test case of an concentrating solar thermal power plant consists 4 parallel absorber tube loops with 48 mirror modules, each 12 m long. The parameters of the optical model for the power plant test case are given in Table 6.

Parameter	Description	Value
G	Aperture width of the mirrors	5.76 m
$\eta_{\text{reflectivity}}$	Optical efficiency of the collector reflectivity	96 %
η_{thermal}	Thermal efficiency of the absorber tube	70 %
r_{absorber}	Radius of the absorber tubes	35 mm
A_{absorber}	Cross sectional area of the absorber tubes	$3.85 \cdot 10^{-3}$ m^2
r_{header}	Radius of the header tubes	20 mm
A_{header}	Cross sectional area of the header tubes	$1.26 \cdot 10^{-3}$ m^2
N_{m}	Number of the modules per absorber tube	48
l_{m}	Length of a module	12 m
l_{absorber}	Total length of the absorber tube ($N_{\text{m}} \cdot l_{\text{m}}$)	576 m
l_{header}	Distance between inflow valves of the header tube	30 m
N	Number of parallel absorber tubes	4
α	Absorbance of the absorber tube	95 %
γ	Transmittance of the tube metal	95 %
l_{row}	Row shadowing	0.6059 m

Table 6: Parameters of the optical model for the power plant test case

4.2 Network with single collector row

In this subsection, the control schemes are tested on the test cases for the network with a single collector row and the results are shown. It starts from the design point and compares the mirror control and valve control with partial shadowing.

4.2.1 Design point

A design point with constant solar irradiation and constant valves' opening state is used, such that the heat transfer fluid reaches exactly the desired outflow temperature at the end of each absorber tube.

The full intensity of direct solar irradiation is assumed while not any clouds overshadowing the collectors are considered. The heating temperature reaches exactly the desired outflow temperature of 666.35 K. The volumetric flow through the tube is 27.18 m^3h^{-1}, which is 7 % higher than the measured value at this time point at 25.3 m^3h^{-1}. The behavior of the temperature in the absorber tube results in a straight line since the temperature rises evenly and strictly monotonously due to the constant solar irradiation and the constant pump flow, see Figure 4. This design point serves as the start point for the following test case scenarios.

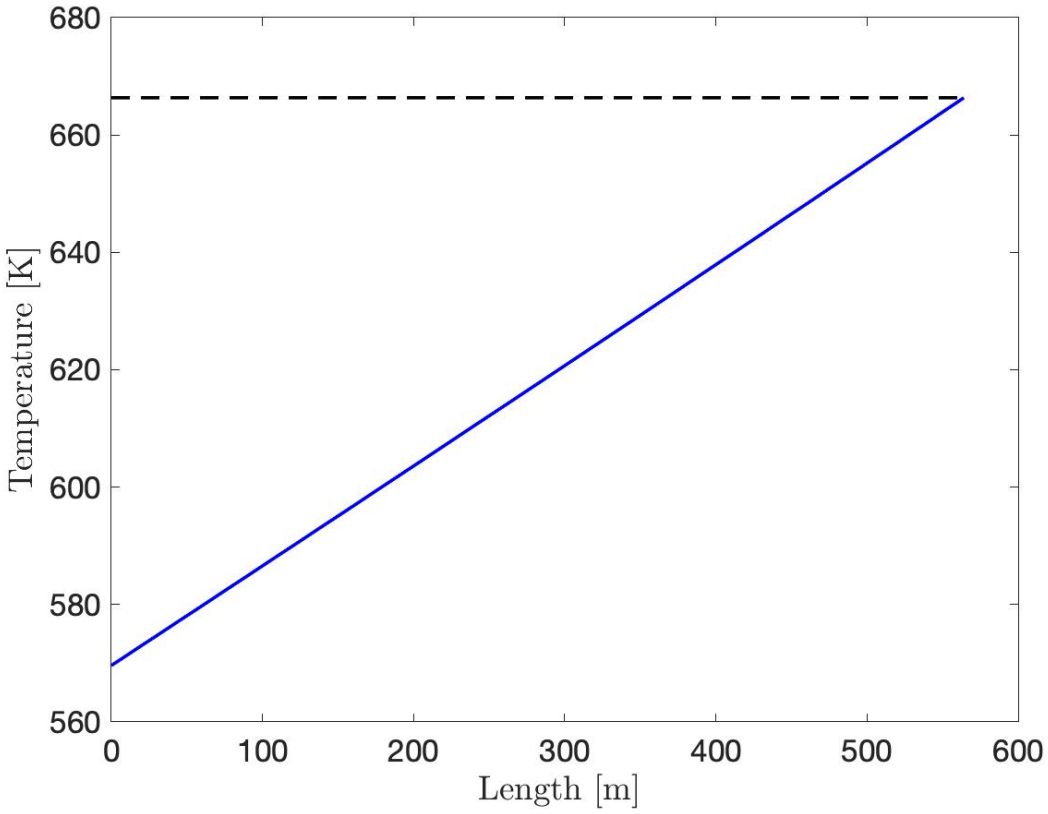

Figure 4: The behavior of the temperature in the absorber tube with no partial shadowing for the design point. The temperature increases over the length of the tube and reaches exactly the desired temperature.

4.2.2 Mirror control

To testing the control schemes, shadows were simulated over the collector row. The shadow distribution is from mirror 30 to 35. Once the mirror is overshadowed, the solar irradiation was set to zero over these parts. In the not overshadowed parts, the collector row stays constant with the value used to calculate the design point.

The mirror control is tested on the single partially overshadowed absorber tube.

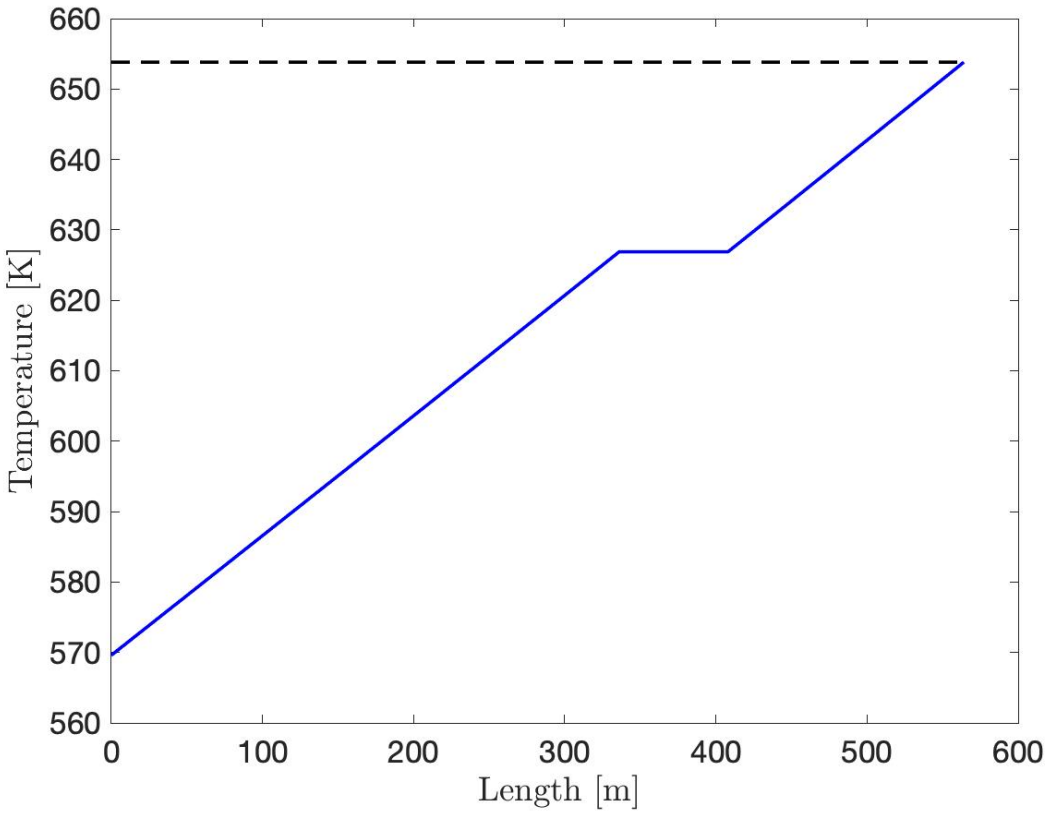

Figure 5: The behavior of the temperature in a single absorber tube with partial shadowing for the mirror control mechanism. In the overshadowed parts the temperature does not increase because the solar irradiation was set to zero. The pump volumetric flow was decreased to reach the desired temperature.

Figure 5 shows that in the overshadowed parts of the tube the temperature keeps constant since the solar irradiation in these parts is zero. In the not overshadowed parts, the temperature increased slightly steeper to be able to reach the desired temperature. In comparison to the design point, the volumetric flow of the pump q_{pump} was decreased to 21.69 m^3h^{-1} to slow the flow of the HTF. This is due to the lower energy input caused by overshadowing. The simulation took 79.6274 seconds.

4.2.3 Valve control

To compare the results of the valve control and mirror control, the same setting of the overshadowed collector row is used. The expectations of the results are also the same. In the overshadowed parts the temperature should keep constant. Unfortunately, the simulation has failed to meet expectations, see Figure 6. There must be a bug in the implementation. The volumetric flow is 12.32 m^3h^{-1} and the outlet temperature is 665.35 K. The volumetric flow is 43 % lower than the volumetric flow achieved by the

mirror control. The reason for the difference is that the valve control can reach the desired temperature exactly, while the volumetric flow has to be decreased.

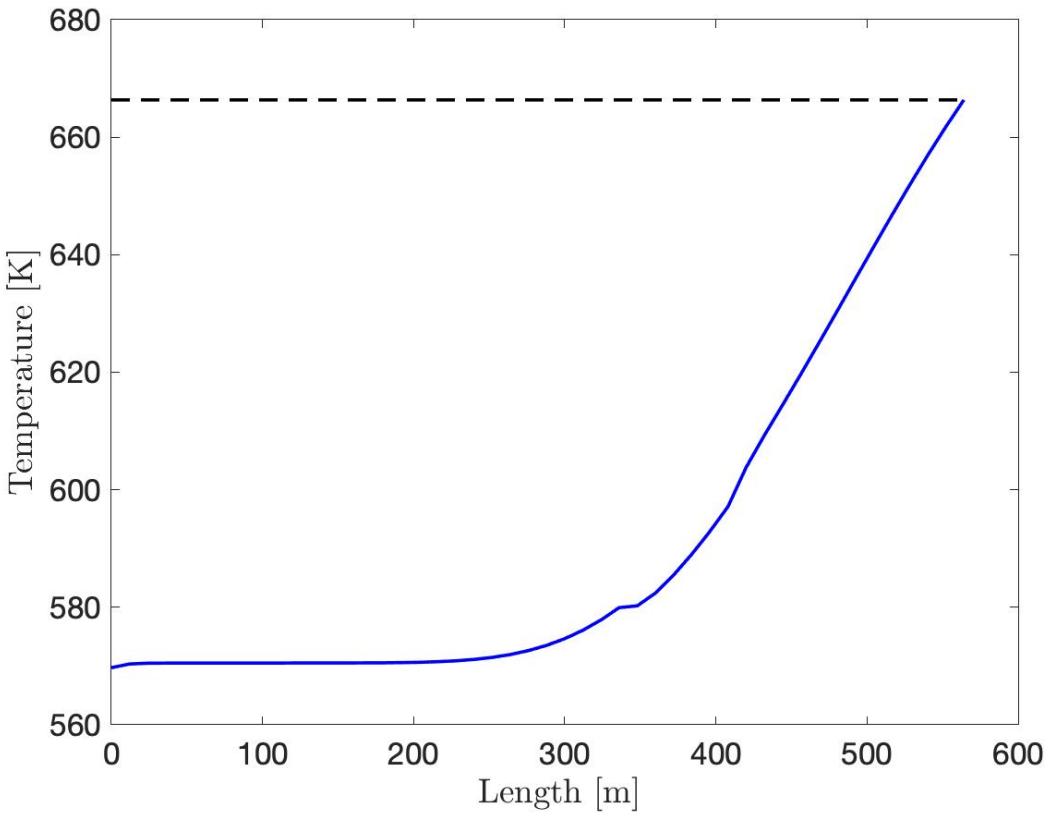

Figure 6: The behavior of the temperature in a single absorber tube with partial shadowing to the valve control mechanism. The pump volumetric flow was decreased to reach the desired temperature.

4.3 Network with four collector rows

In this subsection, the control schemes are tested on the test cases for the network with four absorber tubes and the results are shown. It starts from the design point again and compares the mirror control and valve control with partial shadowing.

4.3.1 Design point

The valves and the volumetric flow of the pump have to be set for the simulation of the design point for a network of tubes. The volumetric flow through each absorber tube should be the same. As a result of this, the increase in temperature should also be the same.
Figure 7 shows the temperature behavior for a solar thermal power plant with four

collector rows without partial shadowing. The power plant is set to a design point where all four absorber tubes could reach the desired temperature. The volumetric flow of 108.18 m^3h^{-1} is the maximum flow the plant can reach with the solar irradiation shown in Table 6.

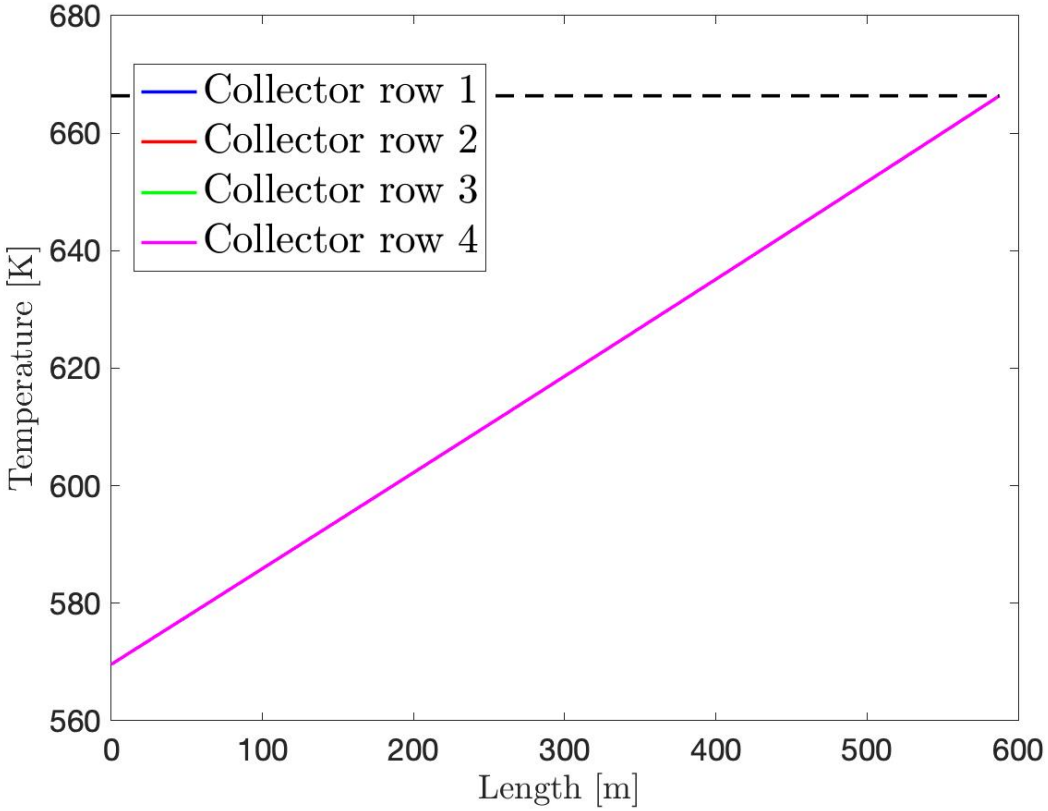

Figure 7: The behavior of the temperature in each absorber tube for the design point. The temperatures behave in the same way in all four rows.

4.3.2 Mirror control

In this test case, the mirror control is used to control the temperature in the network with four absorber tubes. The shadow distribution of the second tube is from mirror 1 to 3 and 10 to 20. The shadow distribution of the third tube is from mirror 1 to 5 and 15 to 23. The shadow distribution of the third tube is from mirror 1 to 17. Once the mirror is overshadowed, the solar irradiation was set to zero over these parts. In the not overshadowed parts, the collector row stays constant with the value used to calculate the design point. As can be seen in Figure 8 the overshadowed parts of the collector field represent a horizontal course of the temperature. The fewer the tube is overshadowed, the more mirrors must be defocused to keep the temperature inside the desired interval. However, the simulation results have failed to meet the

expectation, since not all four tubes reach the desired temperature. The volumetric flow of 70.21 m^3h^{-1} is significantly lower than the volumetric flow of the design point. This difference is caused by the energy loss of the overshadowed parts of the collector field and the defocused mirrors. The outlet temperature of the first collector row at the end of the network is 653.82 K, which is slightly lower than the desired temperature. This is due to that the temperature is kept in a certain interval to ensure it under the desired temperature.

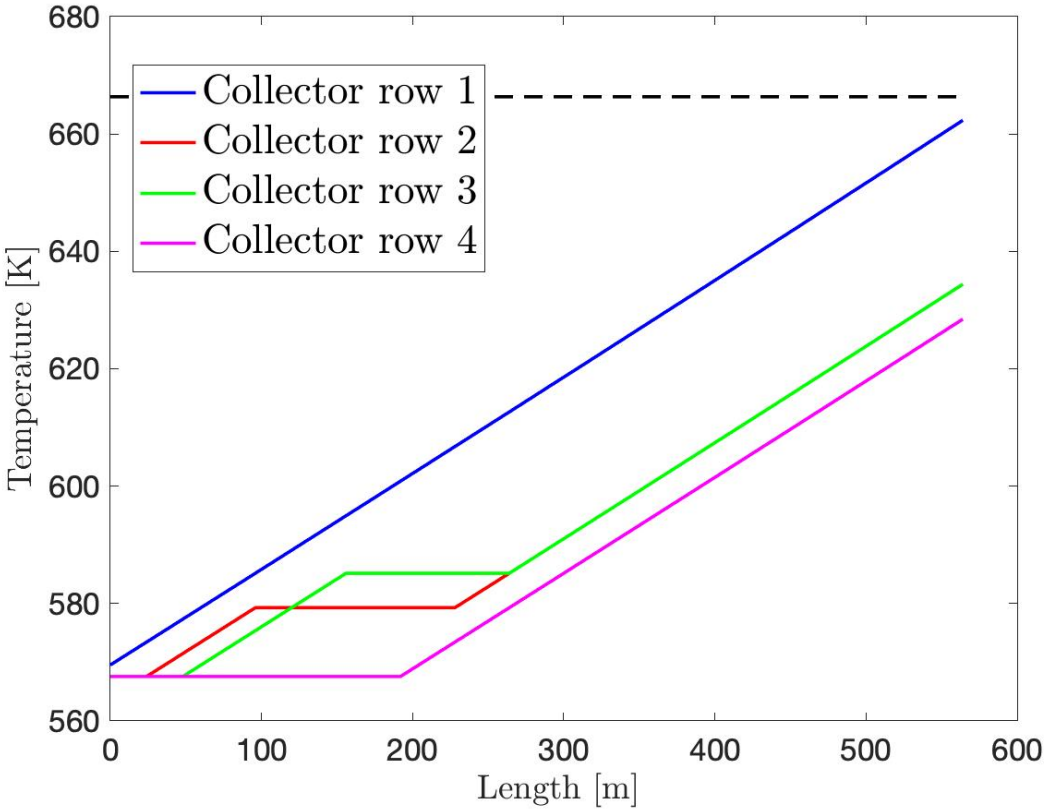

Figure 8: The behavior of the temperature in each absorber tube with partial overshadowing and the valve control mechanism. Not all four tubes reach the desired temperature. In every tube, enough mirrors are defocused so that they do not exceed the maximum temperature.

4.3.3 Valve control

To testing the control schemes, shadows were simulated over the collector row. In this test case, the valve control is used to control the temperature in the network with four absorber tubes. As showed in the previous section, every tube is overshadowed in a different way and a different length. If no mirror is defocused, this would lead to that each tube reaches a different temperature. The valve control controls the volumetric

through each absorber tube separately, so that the temperature distribution along each absorber tube is expected to be different. This results that the course of the temperatures in the absorber tubes should not be parallel. The overshadowed parts of the collector field represent a horizontal course of the temperature. Since no mirrors were defocused and the volumetric flow through each tube was controlled separately, the desired temperature should reach in all tubes. To achieve the desired temperature exactly, the gradients of the temperature distributions in each absorber tube should be different. Unfortunately, there should be a bug in the implementation, such that the simulation does not return a useful result. However, it can be expected that both the temperature and the volumetric flow at the heat exchanger should increase using the valve control compared to the mirror control. It should be a significant improvement to the efficiency of the solar thermal power plant, since the energy loss comes only from the overshadowing parts of the collector field.

5 Conclusion

Within this thesis, several control strategies are introduced to control the heat transfer fluid's temperature at the end of each absorber tube of a parabolic trough solar thermal power plant. The optics of the solar field, the thermodynamics in the tubes, and the flow in a network of tubes are modeled. The state of the art control method is extended by controlling each valve at the inlet of each absorber tube independently. Two test cases are constructed from a real dataset to verify the implementation and compare the results. According to the comparison, we can see that the valve control results in a higher volumetric flow of the heat transfer fluid over the approach of defocussing mirrors when using a solar thermal power plant. This shows that the valve control is more efficient than mirror control. Although the result of the simulation has failed to meet the expectation, the valve control should have higher efficiency than the mirror control since the whole available solar thermal energy is used by using the valve control.

Since in real practice it is hard to adjust the valves so precisely as mentioned in the course of simulations, the next step would have to include the so-called sliding shutter valves. This can be realized by a kind of staircase function that represents the valve setting. Furthermore, a more accurate thermodynamic model considering the pressure drop inside the network of tubes would be conceivable. Moreover, the quality of a control method is highly dependent on the prediction accuracy of the cloud. Therefore, it is important to investigate its sensitivities regarding uncertainties.

References

[1] Walter Benenson, John W Harris, Horst Stöcker, and Holger Lutz. *Handbook of physics*. Springer Science & Business Media, 2006.

[2] John J Burkhardt III, Garvin A Heath, and Craig S Turchi. Life cycle assessment of a parabolic trough concentrating solar power plant and the impacts of key design alternatives. *Environmental science & technology*, 45(6):2457–2464, 2011.

[3] AJ Calvaer. *Power Systems: Modelling and Control Applications: Selected Papers from the IFAC Symposium, Brussels, Belgium, 5-8 September 1988*. Elsevier, 2014.

[4] Eduardo F Camacho and Manuel Berenguel. Control of solar energy systems. *IFAC Proceedings Volumes*, 45(15):848–855, 2012.

[5] M. Cherek. Regulating the temperature in a network of tubes in solar thermal power plants. Bachelor thesis, RWTH Aachen University, 2018.

[6] LL Chung, Yen-Po Wang, and CC Tung. Instantaneous control of structures with time-delay consideration. *Engineering structures*, 19(6):465–475, 1997.

[7] Russell Forristall. Heat transfer analysis and modeling of a parabolic trough solar receiver implemented in engineering equation solver. Technical report, National Renewable Energy Lab., Golden, CO.(US), 2003.

[8] AJ Gallego and EF Camacho. Adaptative state-space model predictive control of a parabolic-trough field. *Control Engineering Practice*, 20(9):904–911, 2012.

[9] Michael Geyer, Eckhard Lüpfert, Rafael Osuna, Antonio Esteban, Wolfgang Schiel, Axel Schweitzer, Eduardo Zarza, Paul Nava, Josef Langenkamp, Eli Mandelberg, et al. Eurotrough-parabolic trough collector developed for cost efficient solar power generation. In *11th International symposium on concentrating solar power and chemical energy technologies*, pages 04–06, 2002.

[10] Andrea Giostri. *Transient effects in linear concentrating solar thermal power plant*. PhD thesis, Italy, 2014.

[11] Michael Hinze. Instantaneous closed loop control of the navier–stokes system. *SIAM journal on control and optimization*, 44(2):564–583, 2005.

[12] Eckhard Lüpfert, Eduardo Zarza, Michael Geyer, Paul Nava, Josef Langenkamp, Wolfgang Schiel, Antonio Esteban, Rafael Osuna, and Eli Mandelberg. Euro trough collector qualification complete-performance test results from psa. In *ISES Solar World Congress 2001 & 2003 Proceedings*, 2003.

[13] Anthony S McCormack and Keith R Godfrey. Rule-based autotuning based on frequency domain identification. *IEEE transactions on control systems technology*, 6(1):43–61, 1998.

[14] Sarah Mechhoud and Taous-Meriem Laleg-Kirati. Source term boundary adaptive estimation in a first-order 1d hyperbolic pde: Application to a one loop solar collector through. In *American Control Conference (ACC), 2016*, pages 5219–5224. IEEE, 2016.

[15] MJ Montes, A Abánades, JM Martínez-Val, and M Valdés. Solar multiple optimization for a solar-only thermal power plant, using oil as heat transfer fluid in the parabolic trough collectors. *Solar energy*, 83(12):2165–2176, 2009.

[16] J Ignacio Ortega, J Ignacio Burgaleta, and Félix M Téllez. Central receiver system solar power plant using molten salt as heat transfer fluid. *Journal of Solar energy engineering*, 130(2), 2008.

[17] Ricardo Vasquez Padilla. *Simplified methodology for designing parabolic trough solar power plants*. University of South Florida USA, and Universidad del Norte, Baranquilla ..., 2011.

[18] Robert Pitz-Paal, Jürgen Dersch, Barbara Milow, Felix Tellez, Alain Ferriere, Ulrich Langnickel, Aldo Steinfeld, Jacob Karni, Eduardo Zarza, and Oleg Popel. Development steps for parabolic trough solar power technologies with maximum impact on cost reduction. 2007.

[19] R. Popp, R. Flesch, T. Konrad, U. Jassmann, and D. Abel. Control-oriented model of a molten salt solar power central receiver. In *2019 18th European Control Conference (ECC)*, pages 2295–2300, 2019.

[20] V Siva Reddy, SC Kaushik, and SK Tyagi. Exergetic analysis and performance evaluation of parabolic trough concentrating solar thermal power plant (ptcstpp). *Energy*, 39(1):258–273, 2012.

[21] Tim Reuscher, Lorenz Pyta, Thomas Konrad, Pascal Richter, and Dirk Abel. Proper orthogonal decomposition and bilinear lyapunov control of parabolic trough collectors. In *2019 27th Mediterranean Conference on Control and Automation (MED)*, pages 439–444. IEEE, 2019.

[22] Elizabeth Saade, David E Clough, and Alan W Weimer. Model predictive control of a solar-thermal reactor. *Solar Energy*, 102:31–44, 2014.

[23] A. Sachtje. Predictive control of the flow in networks of tubes in solar thermal power plants. Master's thesis, RWTH Aachen University, 2019.

[24] M. S. Sohal, M. A. Ebner, P. Sabharwall, and P. Sharpe. Engineering database of liquid salt thermophysical and thermochemical properties. Technical report, Idaho National Laboratory (INL), 2010.

[25] Solutia. Therminol VP-1 Heat Transfer Fluid by Solutia. Technical Bulletin 7239115B, http://www.therminol.com, 2001.